account for the observed changes in τ_0. An even lower sensitivity to a similar temperature increase has been observed for stilbene triplets in several solvents,[12] which may indicate that, in that case, K remains sufficiently large in the 25–100 °C range for τ_0 to be dominated by a temperature independent k_d. A shift of the equilibrium composition toward twisted conformations of the stilbene triplet state can be inferred, however, from an analysis of the temperature dependence of the azulene effect on sensitized cis–trans photoisomerization.[9,33]

The Energy of 2-NPE Triplets. The Sandros plot in Figure 5 indicates an effective energy of ~49 kcal/mol for the lowest *trans*-2-NPE triplets.[20,34] Steady-state measurements indicating that triplet excitation transfer to *trans*-2-NPE is irreversible with fluorenone but reversible with benzanthrone as donor[8] are nicely consistent with this energy. Thus, in addition to strong similarities in decay and quenching behavior, the 2-NPE triplets are very similar to stilbene triplets with respect to energetics.[11,35] This conclusion is consistent with the absorption spectrum of *trans*-2-NPE in ethyl iodide which yielded 53 kcal/mol as an upper limit for its triplet energy.[36] The results clearly show that the lowest 2-NPE triplet states can best be described as substituted olefin triplets rather than as perturbed naphthalene triplets as previously suggested.[36]

It is concluded that the transient kinetic observations confirm several of the key steps of the mechanism proposed for sensitized 2-NPE photoisomerization. Similar measurements using *cis*-2-NPE are planned in order to determine the degree to which the relative population of isomeric triplet states depends on the starting 2-NPE isomer. Isomerization quantum yield measurements, now in progress, may reveal variations of effective α with sensitizer and/or possible excitation transfer inefficiencies in the quenching of sensitizer triplets by the 2-NPE's: cf. ref 37 and 38.

Acknowledgment. We thank Professor Schulte-Frohlinde for stimulating discussions and Mr. L. J. Currell for technical assistance. Work at Florida State University was supported by NSF Grants CHE 77-23582 and CHE 80-26701. D.W.E. thanks the National Science Foundation for a predoctoral graduate research fellowship, 1979–1981.

(33) Saltiel, J.; Rousseau, A. D.; Eaker, D. W., manuscript in preparation.
(34) Sandros, K. *Acta Chem. Scand.* **1964**, *18*, 2355.
(35) Saltiel, J.; Khalil, G.-E.; Schanze, K. *Chem. Phys. Lett.* **1980**, *70*, 233.
(36) Hammond, G. S.; Shim, S. C.; Van, S. P. *Mol. Photochem.* **1969**, *1*, 89.
(37) Caldwell, R. A.; Gajewski, R. P. *J. Am. Chem. Soc.* **1971**, *93*, 532.
(38) Valentine, D., Jr.; Hammond, G. S. *J. Am. Chem. Soc.* **1972**, *94*, 3449.

Liquid Crystalline Solvents as Mechanistic Probes. 6. Dynamic Quenching of Pyrene Fluorescence by 5α-Cholestan-3β-yldimethylamine in the Liquid Crystalline and Isotropic Phases of a Cholesteric Solvent†[1]

Valerie C. Anderson, Bruce B. Craig, and Richard G. Weiss*

Contribution from the Department of Chemistry, Georgetown University, Washington, D.C. 20057. *Received March 30, 1981. Revised Manuscript Received May 28, 1981*

Abstract: A method is described for determining the specificity of quenching of pyrene singlets by a tertiary alkylamine, 5α-cholestan-3β-yldimethylamine (CA), in a nonpolar cholesteric liquid crystalline solvent [59.5/15.6/24.9 (w/w/w) cholesteryl oleate/cholesteryl nonanoate/cholesteryl chloride]. It is found that the pyrene–amine orientation for quenching resembles closely the probable exciplex geometry. Activation parameters for the quenching process are phase dependent: from Stern–Volmer derived quenching rate constants at low CA concentrations, the Arrhenius activation energies and preexponential factors in the cholesteric phase are calculated to be $E_6 = 9.9 \pm 0.2$ kcal mol^{-1} and $A_6 = (2.1 \pm 1.3) \times 10^{14}$ M^{-1} s^{-1}; the isotropic phase has $E_6 = 5.3 \pm 0.1$ kcal mol^{-1} and $A_6 = (1.8 \pm 0.4) \times 10^{11}$ M^{-1} s^{-1}. The value of E_6(cholesteric) is found to change with CA concentration, approaching E_6(isotropic) at high CA. A cohesive explanation of these and other results, including the previously reported photodimerization of acenaphthylene in a different cholesteric phase, is advanced.

The mechanism responsible for quenching excited singlet states of aromatic molecules by amines has been investigated extensively during the last several years.[2] Of particular interest has been the specific orientation between the lumophore and amine required for efficient quenching and those factors which lead to stable lumophore–amine excited-state complex (exciplex) formation.

The appearance of a new, red-shifted emission attributed to an exciplex accompanies the quenching of fluorescence of pyrene (P) by alkyl tertiary amines in several solvents of very different viscosity and polarity (usually $\epsilon < 8$). A large part of the exciplex stability can be ascribed to excited pyrene–amine charge-transfer interactions. The accepted geometry for the exciplex[3] places the orbital for the nitrogen lone pair of electrons directly above the π lobes of pyrene. Although specific in orientation, the interaction need not be axially symmetric as depicted in E.

The eventual fate of the exciplex is determined by its stabilization energy which mediates dissociation and by the availability of chemical and photophysical pathways (e.g., electron transfer to form separated ion radicals, intersystem crossing leading to triplets of pyrene and dissociated ground-state amine, and emission

† Dedicated to George S. Hammond on the occasion of his 60th birthday.

(1) Part 5: Cassis, E. G., Jr.; Weiss, R. G. *Photochem. Photobiol.*, submitted for publication.
(2) See for instance: (a) Gordon, M., Ware, W. R., Eds., "The Exciplex"; Academic Press: New York, 1975. (b) Birks, J. B. "Photophysics of Aromatic Molecules"; Wiley-Interscience: London, 1970. (c) Mataga, N.; Ottolenghi, M. In "Molecular Association"; Foster, R., Ed.; Academic Press: London, 1979; Vol. 2, Chapter 1.
(3) (a) Taylor, G. N.; Chandross, E. A.; Schiebel, A. H. *J. Am. Chem. Soc.* **1974**, *96*, 2693. (b) Nakashima, N.; Mataga, N.; Ushio, F.; Yamanaka, C. *Z. Phys. Chem.* **1972**, *79*, 150. (c) Meeus, F.; Van der Auweraer, M.; Dederen, J. C.; De Schryver, F. C. *Recl. Trav. Chim. Pays-Bas* **1979**, *98*, 220.

0002-7863/81/1503-7169$01.25/0

and nonradiative decay which return both pyrene and amine to their ground states). Competition among these is affected by solvent polarity, solvent viscosity, and temperature.

In this work, we have followed the dynamic quenching of pyrene fluorescence by a sterically hindered tertiary amine, 5α-cholestan-3β-yldimethylamine (CA), in the isotropic and cholesteric liquid crystalline phases of a 59.5/15.6/24.9 (w/w/w) mixture of cholesteryl oleate/cholesteryl nonanoate/cholesteryl chloride (CM). The constraints imposed by the matrix of the cholesteric phase allow the dependence of the efficiency of aromatic singlet quenching (and exciplex formation) on the position of the nitrogen lone-pair orbital to be probed. On the basis of solvent order and the molecular shapes of pyrene and CA, quenching in the cholesteric phase of CM should be more difficult than in its isotropic phase *if* the pyrene–CA spatial requirements for exciplex formation (as in E) and fluorescence quenching are similar. On the other hand, quenching efficiency should be solvent phase independent if the effective pyrene–CA collisional orientations are relatively nonspecific. We find that the fluorescence quenching is less efficient in the liquid crystalline phase than in the isotropic phase. A simple explanation of these results requires that the orientations between pyrene and CA necessary for fluorescence quenching and for exciplex formation be similar.

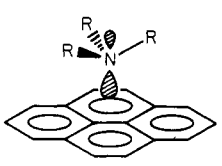

E

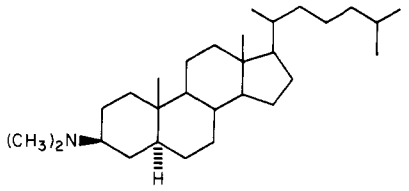

CA

Experimental Section

Melting points and transition temperatures (corrected) were obtained on a Kofler micro hot-stage microscope with polarizing lenses. Boiling points are uncorrected.

Pyrene (Aldrich, 99+%), recrystallized twice from ethanol, mp 150–151 °C (lit.[4] mp 152–153 °C), displayed strictly single exponential fluorescence decays and fluorescence spectra which were indistinguishable from those in the literature.[5] Triethylamine (Aldrich) and tri-*n*-butylamine (Aldrich) were purified by the method of Van and Hammond[6] to give colorless liquids, bp 88.5 °C (lit.[7b] bp 89.5 °C) and 213 °C (lit.[7b] bp 216.5 °C), respectively. Cholesteryl nonanoate (Aldrich), recrystallized from 2-butanone/95% ethanol, exhibited an enantiotropic cholesteric phase from 77.5 to 91 °C (lit.[8a] smectic to cholesteric 77.5, 76.3 °C; lit.[8b] cholesteric to isotropic 92, 92.1 °C). Cholesteryl chloride (PCR) was recrystallized several times from acetone and exhibited a monotropic cholesteric phase with mp 96–97 °C (lit.[9a] mp 95.7, lit.[9b] mp 96.5 °C). Cholesteryl oleate (Aldrich, 97%) was purified by irradiating 8.1 g in 45 mL of nitrogen-saturated heptane with a Hanovia 450-W medium-pressure mercury lamp in a quartz vessel. Nitrogen bubbling was continued during the 21-h irradiation period. The solution was evaporated under reduced pressure and a benzene solution of the resultant solid chromatographed on silica. The benzene eluant was evaporated, and the white solid was recrystallized twice from ether/95% ethanol to yield 4.5 g (55%) of cholesteryl oleate which exhibited an enantiotropic cholesteric phase from 42.5 to 57 °C. Using (presumably) less pure material, previous workers reported a monotropic phase and mp 50.5 °C for the oleate.[10]

5α-Cholestan-3β-yldimethylamine. 5α-Cholestan-3-one (Sigma), 5 g (0.01 mol), and 4.2 g (0.05 mol) of dimethylamine hydrochloride (recrystallized twice from ethanol) were added to a solution containing 190 mL of dry methanol and 0.82 g (0.01 mol) of sodium cyanoborohydride. The mixture was stirred for 110 h. The solvent was removed, and the resultant gray solid was added to a solution of 30 mL of 2 N HCl in 100 mL of water and thoroughly extracted with ether. The aqueous layer was made basic and extracted three times with ether. The combined ether extracts were washed five times with water, dried ($MgSO_4$), and concentrated to give 1.7 g (40%) of a waxy solid. The material was recrystallized four times from ether to give 0.085 g (2%) of 5α-cholestan-3β-yldimethylamine, mp 105–106 °C (lit.[11] mp 105–106 °C).

Dynamic Measurements. Samples were mixed and stirred in the isotropic phase of the solvent until homogeneous. Aliquots were placed in 0.4-mm width flat Pyrex capillary tubes which were flame sealed after several heat (to isotropic temperatures)–pump–cool cycles at ca. 0.05 torr. Decay constants were measured by using an Ortec 9200 single-photon counter[12] with an Ino-tech multichannel analyzer hard-wired to a Data General Nova 3 computer. The excitation light ($\tau_{1/2} \simeq 2.5$ ns) was filtered with a Corning No. 737 glass filter (λ_{cutoff} 360 nm) and focused onto the sample cell. Photons emitted from the front surface of the sample were reflected by a rotatable mirror onto an RCA 8850 photomultiplier tube placed at right angles to the excitation light after passing through a 400-nm (10-nm half-width) interference filter. An emission counting efficiency of <5% was maintained to avoid two photon events.[13] The sample holder was thermostated throughout data collection. Temperature was constant to ±0.5 °C as determined by a calibrated thermistor.

No sample decomposition was detected even after very long counting times. Decay constants were routinely measured at progressively higher temperatures and then reproduced at the lower temperatures to ±1 ns. Duplicate analyses on the same sample and on different samples of the same percent loading indicated that the lifetimes were precise to ±1 ns. A 10^{-5} M solution of quinine sulfate in 0.1 N H_2SO_4 gave τ 19.2 ns (lit.[13] τ 19.4 ns).

Steady-State Fluorescence Measurements. Steady-state fluorescence spectra (uncorrected) were recorded on a Perkin-Elmer MPF-2A spectrophotofluorimeter using the opened capillaries from the dynamic studies. The tubes were attached to a thermostated (±0.5 °C) sample holder positioned at 45° to the 310-nm excitation beam and were not moved while the temperature was varied.

Helical Pitch Measurements.[14] Samples of pyrene and varying concentrations of CA were placed between quartz plates (coated and cured with (3-(methylamino)propyl)trimethoxysilane[15]) separated by a 0.025-mm Teflon spacer. Pitch maxima were recorded at 29, 34.5, 40.5, 44, and 48.5 °C with a Cary 14 spectrophotometer and are estimated to be accurate to ±5 nm.

Results and Discussion

Steady-State Measurements. The cholesteric mixture CM exhibits an enantiotropic cholesteric phase from below ambient room temperature to 57 °C. Its density throughout this phase and up to 80 °C varies very slightly from ca. 1 g/cm^3. Addition of 0.26% (1.3×10^{-2} M) pyrene and the highest concentration of CA employed (9.0%, 0.24 M) depresses the cholesteric–isotropic transition temperature by only 4.5 °C. In contrast, addition of tri-*n*-butylamine, TBA, depresses the transition temperature of CM containing 1.3×10^{-2} M pyrene and 0.13 M TBA by 9 °C. The pitch band of the cholesteric phase varied only slightly upon addition of pyrene and CA: undoped CM at 34.5 °C exhibits a reflectance maximum at 485 nm; the largest deviation, to 710 nm, occurs near the transition temperature of the most highly doped sample.

As reported previously,[16] the absolute intensity of pyrene fluorescence in cholesteric phases varies erratically with temperature (Figure 1a), with sample placement in a spectrophoto-

(4) Birks, J. B.; Kazzaz, A. A.; King, T. A. *Proc. R. Soc. London, Ser. A* **1966**, *291*, 556.
(5) (a) Nakajima, A. *Bull. Chem. Soc. Jpn.* **1971**, *44*, 3272. (b) Nakajima, A. *Spectrochim. Acta, Part A* **1974**, *30A*, 860. (c) Nakajima, A. *J. Mol. Spectrosc.* **1976**, *61*, 467.
(6) Van, S. P.; Hammond, G. S. *J. Am. Chem. Soc.* **1978**, *100*, 3895.
(7) (a) Durham, L. J.; McLead, D. J.; Cason, J. In "Organic Syntheses"; Rabjohn, N., Ed.; Wiley: New York, 1963; Coll. Vol. 4, p 555. (b) Fieser, L. F.; Fieser, M. "Reagents for Organic Synthesis"; Wiley: New York, 1967; Vol. 1, p 1189.
(8) (a) Gray, G. W. *J. Chem. Soc.* **1956**, 3733. (b) Ennulat, R. D. *Mol. Cryst. Liq. Cryst.* **1969**, *8*, 247.
(9) (a) Leder, L. B. *J. Chem. Phys.* **1971**, *54*, 4671. (b) Leclerq, M.; Billard, J.; Jacques, J. *C. R. Hebd. Seances Acad. Sci., Ser. C* **1967**, *264*, 1789.
(10) Davies, G. J.; Porter, R. S.; Steiner, J. W.; Small, D. M. *Mol. Cryst. Liq. Cryst.* **1970**, *10*, 331.
(11) Haworth, R. D.; McKenna, J.; Powell, R. G. *J. Chem. Soc.* **1953**, 1110.
(12) (a) Ware, W. R. In "Creation and Detection of the Excited State", Part A; Lamola, A. A., Ed., Marcel-Dekker: New York, 1971; Vol. 1, Chapter 5. (b) Knight, A. E. W.; Selinger, B. K. *Aust. J. Chem.* **1973**, *26*, 1. (c) Lewis, C.; Ware, W. R.; Doemeny, L. J.; Nemzek, T. L. *Rev. Sci. Instrum.* **1973**, *44*, 107.
(13) Yguerabide, J. In "Methods of Enzymology"; Hirs, C. H. W., Timasheff, S. N., Eds.; Academic Press: New York, 1972; Vol. 26, Chapter 24.
(14) (a) Baessler, H.; Labes, M. M. *Mol. Cryst. Liq. Cryst.* **1970**, *6*, 419. (b) Adams, J. E.; Hass, W. E. *Ibid.* **1971**, *15*, 27.
(15) Kahn, F. J. *Appl. Phys. Lett.* **1973**, *22*, 386.
(16) Novak, T. J.; Mackay, R. A.; Poziomek, E. J. *Mol. Cryst. Liq. Cryst.* **1973**, *20*, 213.

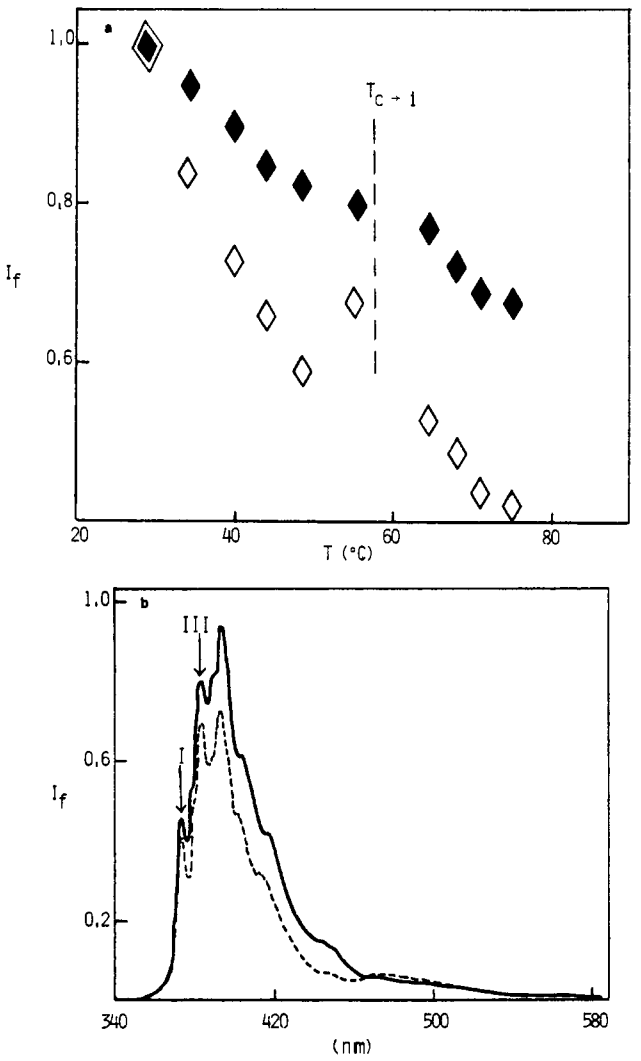

Figure 1. (a) Relative fluorescence intensities at 383 nm normalized to 29 °C for 1.3×10^{-2} M pyrene in the absence (♦) and presence (◇, 0.15 M) of CA. (b) Emission spectra (uncorrected) of 1.3×10^{-2} M pyrene in the absence (–) and presence (- - -, 0.15 M) of CA in CM at 34.5 °C. The intensity ratios of the two spectra are not reflective of the quantum efficiencies.

fluorimeter, and even from sample to sample. These fluctuations are due to surface ordering effects and birefringence of the liquid crystalline media. For these reasons, attempts to construct isothermal Stern–Volmer plots from CA-quenched pyrene fluorescence in the liquid crystalline phase of CM proved futile.

Emission spectra in cholesteric phases are quite well resolved and compare favorably with those obtained for pyrene in isotropic solvents[6] (Figure 1b). The ratio of intensities of bands III to I is a diagnostic for the polarity of the immediate environment in which pyrene fluoresces.[17] The observed ratio in CM, $I_{III}/I_I \simeq 2$, indicates that the pyrene lumophores reside primarily in the hydrocarbon-like part of the cholesteric molecules and away from the ester groups: $I_{III}/I_I = 1.83$ for methylcyclohexane (ϵ 2.02),[17] $I_{III}/I_I = 0.69$ for ethyl acetate (ϵ 6.02),[17] and $I_{III}/I_I = 0.73$ for dichloromethane (ϵ 8.93).[17]

The structureless emission to the red of the monomer fluorescence in Figure 1b is considered to be from the pyrene excimer, although the shape and location of the emission are consistent with those for a pyrene–aliphatic amine exciplex ($\lambda_{max} \simeq 480$ nm).[18] The assignment is substantiated by the lack of

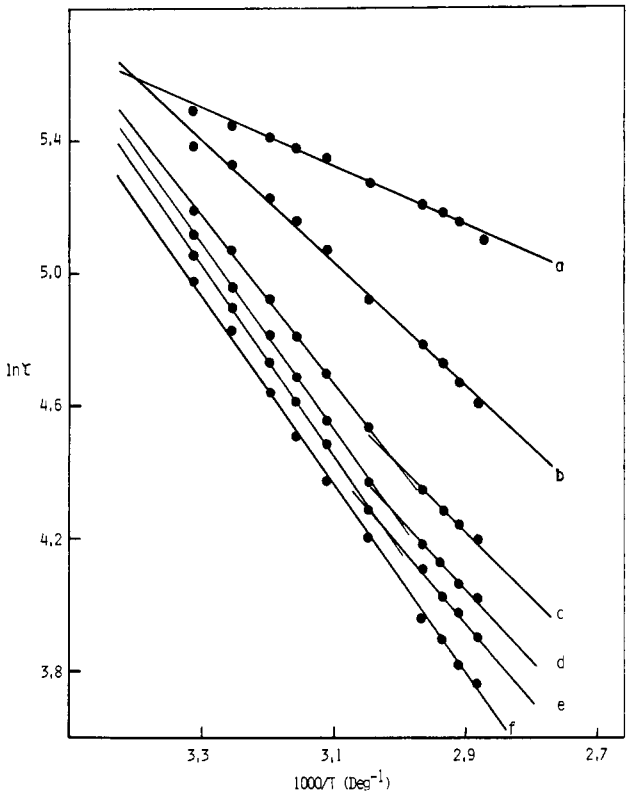

Figure 2. Logarithm of decay constants for pyrene singlets vs. the inverse of temperature in CM for 1.3×10^{-2} M pyrene and CA = 0 M (a), =0.047 M (b), =0.12 M (c), =0.15 M (d), =0.19 M (e), and =0.24 M (f).

increase in the ratio of 480 nm to monomer emission intensities as the CA concentration is changed from 0 to 0.24 M.[19] As expected, pyrene excimer emission spectra recorded in CM in the absence of CA appear at the same wavelengths as found in its presence.

Other aliphatic tertiary amines do form weakly emissive exciplexes with pyrene in isotropic solvents of lower and higher polarity than CM.[18] In fact, emission ($\lambda_{max} \simeq 480$ nm) attributable to an exciplex is observed when either 0.21 M triethylamine or 0.13 M TBA is added to 1.3×10^{-2} M pyrene dissolved in CM (cholesteric and isotropic phases; vide infra).

Dynamic Measurements. Dynamic measurements of pyrene fluorescent lifetimes in a different liquid crystal, cholesteryl benzoate, have been reported[20a] to vary peculiarly with temperature. In our system, this is not the case, and we have not explored the reason for this fortuitous discrepancy.[20b]

Pyrene fluorescence decay curves from single-photon counting experiments were found to remain exponential over at least 3 half-lives when the solvent was either the cholesteric or isotropic phase of CM. The decay constants obtained from semilog plots of emission intensity vs. time from three different regions of each decay curve were found to vary by less than 2 ns and were usually within 1 ns. To avoid interference from the excitation lamp pulse, curve fitting was begun several ($\gtrsim$20) nanoseconds after time zero.

The temperature dependence on the observed lifetimes for 1.3×10^{-2} M pyrene in the cholesteric and isotropic phases of CM is that expected from a viscous isotropic solvent (Figure 2).[21] In the presence of some CA concentrations, a change is observed in

(17) Kalyanasundaraman, K.; Thomas, J. K. *J. Am. Chem. Soc.* **1977**, *99*, 2039.

(18) For pyrene–TBA exciplexes, the emission maximum occurs at 475 nm in heptane and 505 nm in ethyl acetate: Purkayastha, A. K.; Basu, S. *J. Photochem.* **1979**, *11*, 261.

(19) (a) Birks, J. B.; Alwattar, A. J. H.; Lumb, M. D. *Chem. Phys. Lett.* **1971**, *11*, 89. (b) Weyl, D. A. *Spectrochim. Acta, Part A* **1968**, *24A*, 1017. (c) Birks, J. B.; Lumb, M. D.; Munro, I. H. *Proc. R. Soc. London, Ser. A* **1964**, *280*, 289.

(20) (a) Tomkiewicz, Y.; Weinreb, A. *Chem. Phys. Lett.* **1969**, *3*, 229. (b) Measurements made with another cholesteric phase whose pitch band is >23 000 Å (a 10/29/61 [w/w/w] mixture of cholesteryl oleate/cholesteryl nonanoate/cholesteryl chloride) yielded results very similar to those with CM.

(21) Birks, J. B.; Srinivasan, B. N.; McGlynn, S. P. *J. Mol. Spectrosc.* **1968**, *27*, 266.

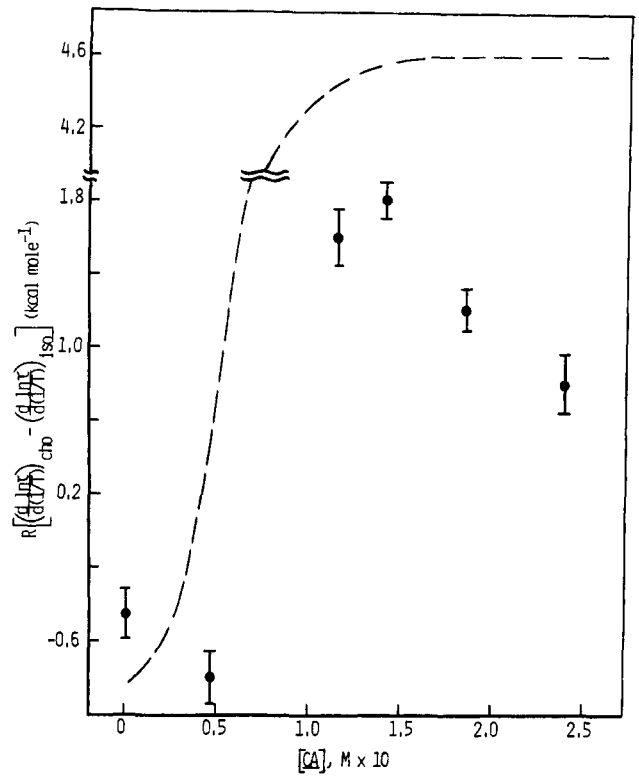

Figure 3. Differences in slopes of cholesteric and isotropic regions of data in Figure 2 multiplied by the universal gas constant vs. CA concentration. The dashed line represents the approximate shape of the curve if E_6 (cholesteric) were independent of concentration.

slope at or near the optically detected solvent transition temperature. However, each of the plots can be fit to no more than two linear slopes. The differences in slopes (displayed as a function of CA concentration in Figure 3), although small, are real and easily reproduced.

Treatment of Data according to a Kinetic Model. A standard mechanism for quenching of excited singlets of pyrene (P^1) by CA is given in Scheme I. Since excimer formation is irreversible ($k_5 \gg k_4$)[19c] and exciplex dissociation is unimportant ($k_8 \gg k_7$; see Appendix), the decay constants for pyrene fluorescence in Figure 2 correspond to τ° and τ, the lifetimes of pyrene singlets in the absence and presence of CA, respectively (eq 8 and 9). In fact, even if k_4 and k_7 were nonnegligible, eq 8 and 9 hold as long as the excimer and exciplex lifetimes are much shorter than the measured lifetime of the pyrene singlets.[22]

Scheme I. Standard Mechanism for Quenching of Pyrene (P) Singlets by CA in a Nonpolar Solvent

$$P \xrightarrow{h\nu} P^1 \quad (1)$$

$$P^1 \xrightarrow{k_1} P + h\nu' \quad (2)$$

$$P^1 \xrightarrow{k_2} P \text{ or } P^3 \quad (3)$$

$$P + P^1 \underset{k_4}{\overset{k_3}{\rightleftharpoons}} (PP)^1 \quad (4)$$

$$(PP)^1 \xrightarrow{k_5} 2P + (h\nu'' \text{ or } \Delta) \quad (5)$$

$$CA + P^1 \underset{k_7}{\overset{k_6}{\rightleftharpoons}} (E)^1 \quad (6)$$

$$(E)^1 \xrightarrow{k_8} P \text{ or } P^3 + CA + (h\nu''' \text{ or } \Delta) \quad (7)$$

$$\tau^\circ = 1/(k_1 + k_2 + k_3P) \quad (8)$$

$$\tau = 1/(k_1 + k_2 + k_3P + k_6CA) \quad (9)$$

$$\tau^\circ/\tau = 1 + k_6\tau^\circ CA \quad (10)$$

Table I. Effects of CA Concentration on the Slopes from Figure 2 as a Function of Phase and on CM Transition Temperatures

[CA],[a] M	$d \ln \tau/d(1/T) \times 10^{-3}$, K: cholesteric[b]	$d \ln \tau/d(1/T) \times 10^{-3}$, K: isotropic[b]	$T_{c\rightarrow i}$,[c] °C
0	0.8 ± 0.04	1.0 ± 0.09	57-57.5
0.047	1.7 ± 0.1	2.1 ± 0.04	56.5-57
0.12	2.5 ± 0.05	1.7 ± 0.1	56.5-57
0.15	2.8 ± 0.03	1.9 ± 0.07	56-56.5
0.19	2.9 ± 0.04	2.3 ± 0.07	55.5-56
0.24	3.0 ± 0.07	2.6 ± 0.1	53-53.5

[a] Pyrene concentration is constant at 0.013 M. [b] From data points within a phase. Errors are standard deviations from linear least-squares fits. [c] CM cholesteric to isotropic transition temperature.

Pyrene excimer lifetimes in saturated hydrocarbon solvents[23] and in CM[24a] are known to meet this condition. Since the exciplex between pyrene and CA is nonemissive, its lifetime could not be measured. However, it can be approximated from the lifetimes of other pyrene–trialkylamine exciplexes which are emissive. In hexane at 21 °C, the lifetime of the exciplex between pyrene and TBA (IP = 7.22 eV[25a]) is reported to be 33 ns.[3b] The lifetime of this exciplex in CM (1.3×10^{-2} M pyrene and 0.13 M TBA) is found to be 11 ± 1 ns at 29 °C (cholesteric phase) and 12 ± 1 ns at 53 °C (isotropic phase). The monomer lifetimes in the cholesteric phase are at least 10 times as great as those of the exciplex under these conditions; in the isotropic phase, they are at least 7 times as great.

If charge transfer is largely responsible for the binding energy of these exciplexes, their stability should be proportional to the amine ionization potentials. Taking cyclohexyldimethylamine (IP ≃ 7.0 eV[25b]) as a model for CA, purely *electronic* considerations lead to the prediction that the pyrene–CA exciplex should be more stable (and, therefore, more likely to be emissive) than the pyrene–TBA exciplex. That no emission is observed in CM from the pyrene–CA exciplex indicates that its lifetime is no greater than that of the pyrene–TBA exciplex.

Figure 2 is an Arrhenius-like plot in which the slopes represent the *apparent* activation energies divided by the gas constant, E_a/R, for pyrene singlet loss. The data are collected in Table I and are displayed in Figure 3. There is no a priori reason why these plots should be linear. That they are,[26] at least within a phase, requires that some of the rate constants in eq 8 and 9 either be small, temperature independent, or vary in a parallel fashion with temperature. In all cases in which two different slopes are observed, the intersection occurs within 4 °C of the optically detected transition temperatures.

(22) (a) Lewis, C.; Ware, W. R. *Mol. Photochem.* **1973**, *5*, 261. (b) Ware, W. R. *Pure Appl. Chem.* **1975**, *41*, 635.

(23) Birks, J. B.; Dyson, D. J.; Munro, I. H. *Proc. R. Soc. London, Ser. A* **1963**, *275*, 575.

(24) (a) Anderson, V. C.; Craig, B. B.; Weiss, R. G., *J. Am. Chem. Soc.*, submitted for publication. (b) It should be mentioned that $(k_1 + k_2)$ has been determined to be 3.2×10^6 s^{-1} (cholesteric) and 3.8×10^6 s^{-1} (isotropic) from experiments in CM with several P concentrations in the absence of CA. With use of these values in eq 16 and 17 the following activation parameters are obtained: $A_3 \simeq 2.3 \times 10^{14}$ M^{-1} s^{-1} (cholesteric) and 9.5×10^{12} M^{-1} s^{-1} (isotropic), $E_3 \simeq 9.3$ kcal/mol (cholesteric) and 7.0 kcal/mol (isotropic), $A_6 \simeq 6.3 \times 10^{13}$ M^{-1} s^{-1} (cholesteric) and 1.4×10^{10} M^{-1} s^{-1} (isotropic), and $E_6 \simeq 8.6$ kcal/mol (cholesteric) and 3.5 kcal/mol (isotropic). Since the changes in solute concentrations affect the solvent order and, therefore, E_3 and A_3, it is unclear which set of E_6 and A_6 from eq 17 are most appropriate. However, since the Arrhenius equation determination of E_6 and A_6 depends upon neither E_3 and A_3 nor $k_1 + k_2$, it is probably a more accurate calculation. Regardless, all of the methods yield similar *differences* between the phases. The significance of these results and further studies on the pyrene excimer in CM will be discussed.[24a]

(25) (a) Nakajima, A.; Akamatu, H. *Bull. Chem. Soc. Jpn.* **1969**, *42*, 3409. (b) Calculated from data in: Kayser, R. H.; Young, R. H. *Photochem. Photobiol.* **1976**, *24*, 395.

(26) The deviations from complete linearity of the data points for the 1.3×10^{-2} M pyrene sample in the absence of CA appear to be real and result from the fact that $k_1 + k_2$ is not very much larger than k_3P at this concentration.

Table II. Activation Parameters Calculated from Figure 2 and Equations 14 and 15 or from Figures 4 and 5

	cholesteric phase[d]			isotropic phase[d]		
	a	*b*	*c*	*a*	*b*	*c*
E_3, kcal mol^{-1}	1.5 ± 0.1	2.5 ± 0.1		3.1 ± 0.1	2.8 ± 0.1	
A_3, M^{-1} s^{-1}	(3.2 ± 0.1) × 10^9	(1.0 ± 0.1) × 10^{10}		(3.4 ± 1.7) × 10^{10}	(2.5 ± 1.1) × 10^{10}	
E_3, kcal mol^{-1}	11.8 ± 0.7	11.4 ± 0.4	9.9 ± 0.2	5.4 ± 1.4	5.5 ± 0.1	5.3 ± 0.1
A_6, M^{-1} s^{-1}	(4.9 ± 4.1) × 10^{15}	(1.9 ± 1.0) × 10^{15}	(2.1 ± 1.3) × 10^{14}	(1.3 ± 1.7) × 10^{12}	(1.8 ± 0.2) × 10^{11}	(1.8 ± 0.4) × 10^{11}
$\Delta S_6^{\ddagger}$, eu			+5 ± 0.6			−10 ± 0.4

[a] Using $A_1 + A_2 = 8 \times 10^7$ s^{-1} and $E_1 + E_2 = 3.0$ kcal mol^{-1} as found in liquid paraffin[32] as solvent; from figure 2 and eq 14 and 15. [b] Using $A_1 + A_2 = 1 \times 10^7$ s^{-1} and $E_1 + E_2 = 1.0$ kcal mol^{-1} as found in cyclohexane[23] as solvent; from figure 2 and eq 14 and 15. [c] From Figures 4 and 5. [d] Error limits are standard deviations of linear least-squares fits and reflect precision.

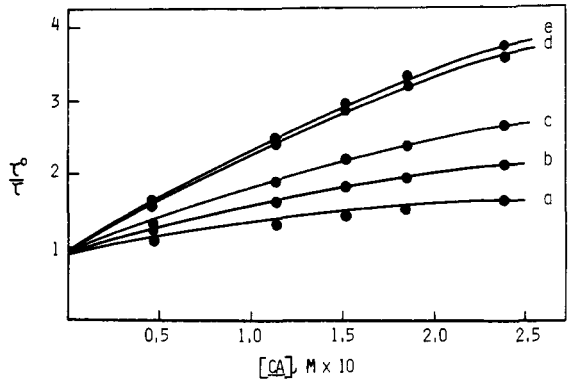

Figure 4. Representative dynamic Stern–Volmer plots for quenching pyrene singlets by CA in the cholesteric (a, 29 °C; b, 40.5 °C; c, 48.5 °C) and isotropic (d, 68 °C; e, 71 °C) phases of CM.

Calculation of Activation Parameters for k_6. The unimolecular rate constants, k_1 and k_2, should be much more dependent upon solvent polarity than viscosity.[27] The bimolecular rate constants, k_3 and k_6, must vary with viscosity if for no other reason than they are proportional to the rate constant for self-diffusion, k_{diff}. (In addition, k_3 and pyrene–alkylamine quenching rate constants analogous to k_6 are known to exhibit nonzero activation energies in isotropic solvents.[23,28]) Therefore, although it should be possible to substitute values of k_1 and k_2 from other nonpolar solvents for those in CM, the k_3 and k_6 must be determined directly from CM data.

In isotropic solvents, k_{diff} is approximated by the Debye equation (eq 11)[29] in which η is the macroscopically measured viscosity in poise. Equation 11 cannot be representative of the diffusion rate constants for pyrene and CA in the liquid crystalline phase of CM for several reasons. The first is that for several CA concentrations, there is no large change in the cholesteric and isotropic phase slopes of ln τ vs. $1/T$ plots (Table I), even though very large (non-Newtonian) viscosity changes are known to occur as cholesteric molecules pass from their liquid crystalline to isotropic phases.[30] The second is that three different orthogonal diffusion rates are expected in the cholesteric liquid crystalline phase.[31] Of these, the one which is measured by normal viscosity methods corresponds to movement of molecules parallel to the helical screw axis.[30] This is not the preferred direction for diffusion of solutes like pyrene and CA (vide infra).

$$k_{diff} = 8RT/3000\eta \qquad (11)$$

The general form of the apparent activation energies, E_a^0 and E_a, follow from describing each of the rate constants in eq 8 and 9 by an Arrhenius expression (eq 12 and 13). Differentiating ln τ with respect to $1/T$ gives eq 14 and 15 which are equal to E_a^0/R and E_a/R, the slopes measured from Figure 2. Thus, eq 16 and 17 hold.

$$\ln \tau = -\ln (k_1 + k_2 + k_3P + k_6CA) \qquad (12)$$

$$\ln \tau = -\ln (A_1e^{-E_1/RT} + A_2e^{-E_2/RT} + A_3Pe^{-E_3/RT} + A_6CAe^{-E_6/RT}) \qquad (13)$$

$$\frac{d \ln \tau^0}{d(1/T)} = \frac{A_1E_1e^{-E_1/RT} + A_2E_2e^{-E_2/RT} + A_3PE_3e^{-E_3/RT}}{R(A_1e^{-E_1/RT} + A_2e^{-E_2/RT} + A_3Pe^{-E_3/RT})} \qquad (14)$$

$$\frac{d \ln \tau}{d(1/T)} = \frac{A_1E_1e^{-E_1/RT} + A_2E_2e^{-E_2/RT} + A_3PE_3e^{-E_3/RT} + A_6CAE_6e^{-E_6/RT}}{R(A_1e^{-E_1/RT} + A_2e^{-E_2/RT} + A_3Pe^{-E_3/RT} + A_6CAe^{-E_6/RT})} \qquad (15)$$

$$E_a^0 = \frac{A_1E_1e^{-E_1/RT} + A_2E_2e^{-E_2/RT} + A_3PE_3e^{-E_3/RT}}{A_1e^{-E_1/RT} + A_2e^{-E_2/RT} + A_3Pe^{-E_3/RT}} \qquad (16)$$

$$E_a = \frac{A_1E_1e^{-E_1/RT} + A_2E_2e^{-E_2/RT} + A_3PE_3e^{-E_3/RT} + A_6CAE_6e^{-E_6/RT}}{A_1e^{-E_1/RT} + A_2e^{-E_2/RT} + A^3Pe^{-E_3/RT} + A_6CAe^{-E_6/RT}} \qquad (17)$$

The sums $A_1 + A_2$ and $E_1 + E_2$ for decay of pyrene singlets can be approximated from data taken in cyclohexane[23] ($A_1 + A_2 \simeq 10^7$ s^{-1}; $E_1 + E_2 \simeq 1$ kcal mol^{-1}) or in the more viscous solvent, liquid paraffin[32] ($A_1 + A_2 \simeq 8 \times 10^7$ s^{-1}; $E_1 + E_2 \simeq 3$ kcal mol^{-1}), since the environment of the pyrene lumophore in CM, as determined from the shape of the monomer fluorescence spectra,[17] is hydrocarbon-like. Internally consistent results were obtained by using the activation parameters from either solvent. For example, substituting $10^7e^{-500/T}$ s^{-1} for $A_1e^{-E_1/RT} + A_2e^{-E_2/RT}$ and $10^7e^{-500/T}$ kcal mol^{-1} s^{-1} for $A_1E_1e^{-E_1/RT} + A_2E_2e^{-E_2/RT}$ in eq 16 and using the actual data points within a phase (at [CA] = 0) allow best-fit values for A_3 and E_3 in each CM phase to be calculated from the data in Table I (see Table II). The E_3 compare favorably with those obtained in cyclohexane[23] (E_3 = 2.3 kcal mol^{-1}), but not in paraffin oil[33] (E_3 = 4.4 kcal mol^{-1}).[24b]

With use of eq 17 and the calculated A_3 and E_3 in Table II, a similar technique yields A_6 and E_6. For these determinations, the data points in Figure 2 for each [CA] ≤ 0.15 M[34] were employed to obtain the best fit of E_6 and A_6. The values at the three CA concentrations were then averaged.

An independent determination of A_6 and E_6 can be obtained from the intercept and slope of an Arrhenius plot (Figure 5), using the k_6 calculated from the limiting slopes ([CA] ≤ 0.15 M) of dynamic Stern–Volmer curves (Figure 4). According to eq 10, the slope of each line in Figure 4 is $k_6\tau^0$. The agreement between

(27) Craig, B. B.; Kirk, J.; Rodgers, M. A. J. *Chem. Phys. Lett.* **1977**, *49*, 437.
(28) Nakashima, N.; Mataga, N.; Yamanaka, C. *Int. J. Chem. Kinet.* **1973**, *5*, 833.
(29) Debye, P. J. *Trans. Electrochem. Soc.* **1942**, *82*, 265.
(30) (a) Sakamoto, K.; Porter, R. S.; Johnson, J. F. *Mol. Cryst. Liq. Cryst.* **1969**, *8*, 443. (b) Porter, R. S.; Barrall, E. M., II; Johnson, J. F. *J. Chem. Phys.* **1966**, *45*, 1452. (c) Pochan, J. M. In "Liquid Crystals: The Fourth State of Matter"; Saeva, F. D., Ed.; Marcel-Dekker: New York, 1979; Chapter 7.
(31) This has been demonstrated in nematic phases: (a) Miesowicz, M. *Nature (London)* **1946**, *158*, 27. (b) Hakemi, H.; Labes, M. M. *J. Chem. Phys.* **1975**, *63*, 3708.
(32) Stevens, B.; Thomăz, M. F.; Jones, J. *J. Chem. Phys.* **1967**, *46*, 405.
(33) Doller, E.; Förster, Th. *Z. Phys. Chem.* **1962**, *34*, 132.
(34) The exclusion of slopes from experiments in which [CA] > 0.15 M is necessitated by decreasing differences in Table I which are related to solute-induced changes in the solvent and, possibly, to other factors mentioned in the text.

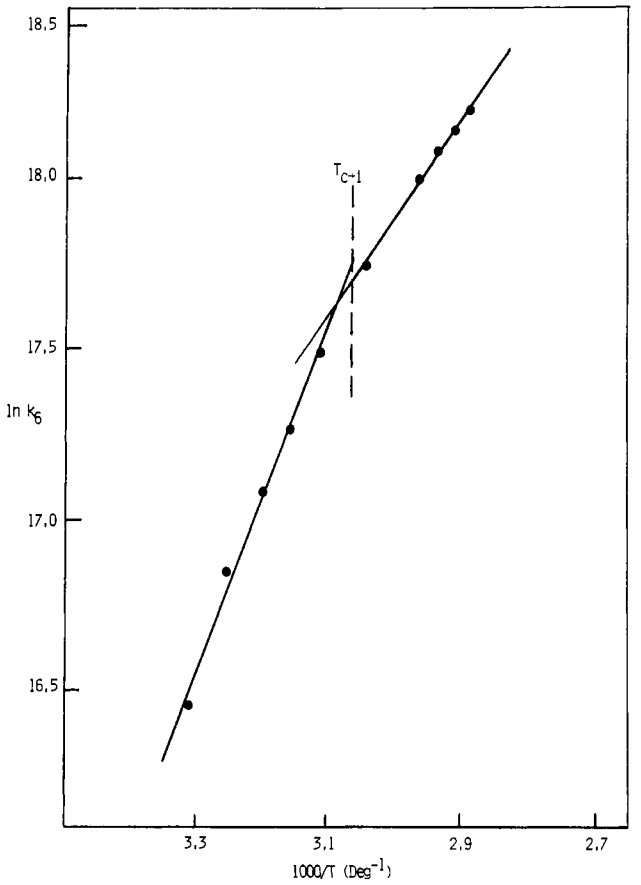

Figure 5. Arrhenius activation plot of ln k_6 vs. the inverse of temperature. The approximate cholesteric to isotropic transition temperature is indicated by the dashed line.

the activation parameters determined in this way and by the best-fit method (assuming k_1 and k_2 values from cyclohexane or liquid paraffin) is astonishing and increases our confidence in their validity.

The downward curvature in the Stern–Volmer slopes at high quencher concentration can indicate significant exciplex dissociation. Plots like Figure 4 have been discussed and treated theoretically in this way by Lewis and Ware.[22] Ground-state aggregation of quencher molecules (eq 18) can also lead to curved

$$n\mathrm{CA} \rightleftharpoons (\mathrm{CA})_n \qquad (18)$$

Stern–Volmer slopes. From the relative lifetimes of P^1 and E, it would appear that exciplex dissociation is not important here. It is unknown whether aggregation or another phenomenon such as solute-induced changes in solvent properties is responsible.

Influence of Solutes on CM. As shown in Table I, not all of the samples with CA display E_a which are very phase dependent. A less drastic concentration dependence has been observed during the photodimerization of acenaphthylene in the cholesteric phase of a 1:1 mixture of cholestanyl acetate and cholestanyl nonanoate.[35] There, addition of successively more tetralin (a solute which disturbs solvent order but does not participate in the photochemistry) or acenaphthylene (up to 0.08 M) resulted in a continuous *decrease* in the quantum efficiency for photodimerization. The decreases with *both* solutes can be attributed to the disordering influence on the cholesteric solvent's order. It is reasonable that CA, in addition to participating in the quenching of pyrene singlets, also disturbs the cholesteric order of CM.

The manifestations of this disordering are opposite in the two studies. In the cholesteric phase of CM, the probability that a pyrene singlet–CA encounter will result in quenching (as measured by the energy barrier, E_6) *increases* as CA concentration is increased. E_6(cholesteric) decreases with increasing CA and becomes very close to E_6(isotropic) at [CA] $\gtrsim$ 0.24 M. This effect is reconcilable with a reasonable model for the positions and mobilities of pyrene and CA within the liquid crystalline phase of CM.

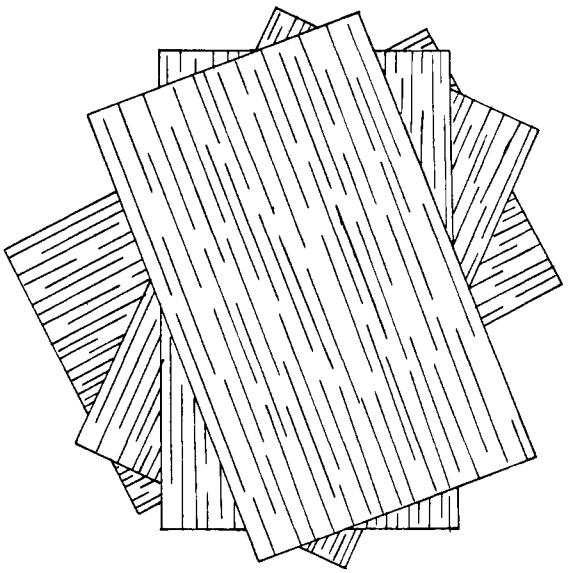

Figure 6. Idealized representation of cholesteric order.

General Medium Considerations. The cholesteric phase of a liquid crystal can be described as a multilayered structure, each layer exhibiting nematic-like order and being twisted with respect to the layers below and above it.[36] The gross effect is to create a macro-helical arrangement like that depicted in Figure 6 in which the average orientation of the long axes within a layer determines the degree of twist or pitch of the helix. Pitch, the distance between layers whose orientations are parallel, is given by $p = \lambda/2n$ where λ is the wavelength of maximum reflectance and n ($\simeq$1.5) is the index of refraction of the medium.[37] As $p \rightarrow \infty$, the phase becomes nematic-like (i.e., the layering vanishes). The pitch band maxima for CM indicate that the pitch varies from ca. 200–300 nm, depending upon temperature and solute concentration, and that the phase remains tightly "wound".

Above the cholesteric–isotropic transition temperature, the long-range order of a cholesteric phase is destroyed. However, some short-range order can persist.[38] Although this short-range order *may* affect the rates and specificities of unimolecular rearrangements and isomerizations (especially those which occur more easily in an ordered phase than in a disordered one), it is unlikely to have a significant impact on the rates and specificities of bimolecular processes which depend upon diffusion. Such a case is found during pyrene fluorescence quenching by CA which occurs more easily in the isotropic phase of CM than in its cholesteric phase.

The preferred direction for diffusion of CA in a cholesteric medium is predicted to be orthogonal to the helical screw axis of the phase. Unfortunately, diffusion rate constants in this plane have not been measured.

The preference for diffusion in these directions can be explained on the basis of crystal packing considerations. Nonpolar solutes like pyrene and CA are most easily accommodated into a cholesteric matrix when their long molecular axes are parallel to the long axes of the constituent solvent molecules.[36] CPK space-filling models of CA and the components of CM indicate that the amine is incorporated into the CM matrix with a small disruption of

(35) Nerbonne, J. M.; Weiss, R. G. *J. Am. Chem. Soc.* **1979**, *101*, 409.

(36) See, for instance, ref 30a. Gray, G. W. "Molecular Structure and Properties of Liquid Crystals"; Academic Press: New York, 1962.

(37) (a) Fergason, J. L. *Mol. Cryst.* **1966**, *1*, 293. (b) Adams, J.; Haas, W. *Mol. Cryst. Liq. Cryst.* **1972**, *16*, 33.

(38) (a) Yang, C. C. *Phys. Rev. Lett.* **1972**, *28*, 955. (b) Cheng, J.; Meyer, R. B. *Phys. Rev. A* **1974**, *9*, 2744. (c) Mahler, D. S.; Keyes, P. H.; Daniels, W. B. *Phys. Rev. Lett.* **1976**, *36*, 491. (d) Crooker, P. P.; Laidlaw, W. G. *Phys. Rev. A* **1980**, *21*, 2174.

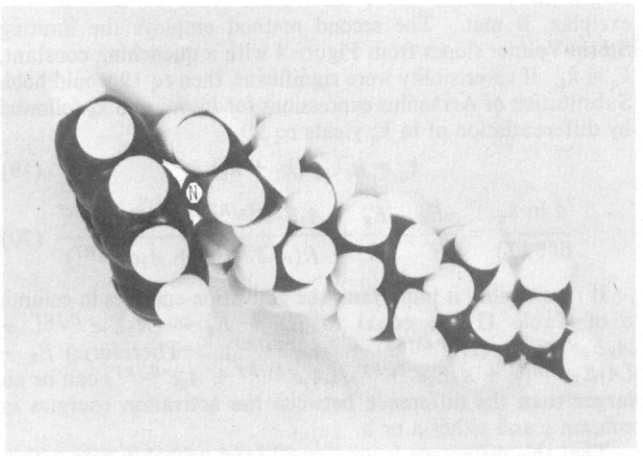

Figure 7. Representation of the pyrene–CA exciplex geometry showing the orientation which allows the greatest proximity of the nitrogen lone-pair orbital to the π lobes of pyrene.

solvent order. This prediction is borne out by the minor changes in pitch and transition temperatures accompanying the addition of CA to CM. Similar experiments with the platelike pyrene show that it has a greater disruptive influence on CM,[24a] although models indicate that pyrene will lie preferentially parallel to or within the solvent layers. Movement of both solutes within the planes defined by the solvent layers will, therefore, be preferred. It should be emphasized that minor changes in the macroscopic properties of a cholesteric phase can mask significant microscopic changes.

Model for Pyrene Singlet Quenching by CA in CM. Aromatic hydrocarbon–amine exciplex formation in nonpolar solvents like CM is thought to require the lone-pair orbital on nitrogen to be perpendicular to and imbedded in the π lobes of the aromatic molecule (E).[3] If the interaction necessary for quenching is less specific, many other collisional orientations between the aromatic molecule and amine ought to be effective, and the quenching rates should be directly proportional to k_{diff}. In this case, the difference in the A_6 for the cholesteric and isotropic phases will be strongly dependent upon the activation parameters for their self-diffusion rates. Although the rates of self-diffusion are not known for CM in the preferred directions of solute movement, it is reasonable to assume that they increase with increasing temperature. Although a diffusion-controlled model may be consistent with E_6(cholesteric) > E_6(isotropic), it does not account for A_6(cholesteric) being *greater* than A_6(isotropic).

A more specific model requires that exciplex structure (E) and the most effective orientations for quenching be similar in nonpolar media.[39] In this case, the favored orientations for collision between pyrene and CA in the cholesteric phase of CM cannot lead to quenching: only when pyrene and CA are tilted with respect to one another is the appropriate electronic interaction possible (Figure 7). Such a tilt would increase the bulkiness of the complex, making it larger in the direction parallel to the helical screw axis. The cholesteric phase of CM, therefore, would become more disordered in the vicinity of the complex as it formed. Inhibition to the tilt by the solvent matrix would make E_6(cholesteric) > E_6(isotropic) while A_6(cholesteric) would be greater, also, due to the disruption of solvent order in the transition state. The activation parameters in Table II are clearly more consistent with this model.

The degree of inhibition by CM to the out-of-plane tilt will be determined by the order of its cholesteric phase. As the concentration of CA is increased, the solvent will become less ordered, approaching the isotropic phase in its *microscopic* properties. Thus, increasing CA concentration serves two functions: to facilitate the orientations of pyrene and CA which can lead to fluorescence quenching by disrupting solvent order and to increase the rate of collisions with pyrene singlets by increasing the statistical probability for collision per unit time. The first results in an increase in the number of encounters between pyrene singlets and CA which lead to quenching and the second increases the number of those encounters. In this way, the CA concentration affects not only the rate of pyrene singlet quenching *but also alters* k_6, *the rate constant for quenching* in the cholesteric phase.

During the photodimerization of acenaphthylene, increased solute concentrations *decreased* the quantum efficiency (and the fraction of effective collisions) for photodimerization since, in that case, the most favored collisional orientations for reaction are those which occur most easily in a very ordered cholesteric phase.[35,41] In the present study, the effect of increased solute concentration on quenching efficiency is exactly the opposite since cholesteric order inhibits quenching. As the order decreases, quenching is facilitated and E_6(cholesteric) decreases, approaching the value obtained in the isotropic phase of CM.

The curvature in Figure 3 is easily reconciled by this model. At 0.013 M pyrene and very low CA concentrations, $k_1 + k_2$ is greater than k_6CA or k_3P, and the apparent E_a of eq 17 is dominated by the order-insensitive unimolecular terms. As the concentration of CA increases, the influence of the order-sensitive bimolecular terms containing CA becomes greater, making the difference between E_a(cholesteric) and E_a(isotropic) more apparent: when $A_6\mathrm{CA}e^{-E_6/RT} > A_1e^{-E_1/RT} + A_2e^{-E_2/RT} + A_3\mathrm{P}e^{-E_3/RT}$ and $A_6\mathrm{CA}E_6e^{-E_6/RT} > A_1E_1e^{-E_1/RT} + A_2E_2e^{-E_2/RT} + A_3\mathrm{P}E_3e^{-E_3/RT}$, $E_a \rightarrow E_6$. If E_6(cholesteric) were, like E_6(isotropic), to remain constant as CA is increased, E_a(cholesteric) − E_a(isotropic) would reach an asymptotic limit approximated by the dotted line in Figure 3 rather than decrease. In fact, the slope of Figure 3 at very large concentrations of CA is predicted to approach zero and be independent of A_6(cholesteric) which may be varying concurrently.

That the difference between E_a(cholesteric) and E_a(isotropic) *does* decrease above 0.15 M CA must be a consequence of a decrease in E_a(cholesteric) which accompanies $E_a \rightarrow E_6$. It cannot be a consequence of exciplex dissociation since the monomer decay times remain much longer than the exciplex decay time.

Activation Parameters for k_6. As expected, the specificity of pyrene singlet quenching by CA results in a negative entropy of activation within the isotropic phase of CM. The E_6(isotropic) is ca. 2 kcal mol^{-1} higher than that found for pyrene singlet quenching by TBA in a nonviscous, nonpolar solvent, hexane.[3b] The difference between the two reflects the greater steric hindrance in CA and the higher viscosity of isotropic CM.

A second piece of evidence for the greater steric hindrance of CA comes from the observation of emission attributable to a pyrene–TBA exciplex in the cholesteric and isotropic phases of CM under conditions where no pyrene–CA exciplex emission was detected (0.13 M TBA). It is possible that the lone pair on nitrogen in TBA is more accessible than in CA, facilitating and stabilizing exciplex formation.

The higher E_6 and more positive entropy of activation found in the liquid crystalline phase of CM are consistent with a very specific, bulky transition state for pyrene singlet quenching by CA. As discussed previously, the more positive entropy of activation arises due to disruption of the order in nearby solvent molecules as the transition state is attained. The larger E_6(cholesteric) than E_6(isotropic) can be attributed to the greater viscosity of CM in its cholesteric phase and to the necessity of the nearby solvent molecules to adopt a thermodynamically less stable arrangement upon formation of the pyrene singlet–CA transition state. The exact contribution of each factor is unknown[42] and must await the measurement of the self-diffusion rates for

(39) As a consequence, a collision complex which precedes exciplex formation must not be catalyzing intersystem crossing[40] or internal decay of the pyrene singlets in nonpolar solvents.

(40) Delouis, J. F.; Delaire, J. A.; Ivanoff, N. *Chem. Phys. Lett.* **1979**, *61*, 343.

(41) An analogous effect is observed during pyrene excimer formation.[24a]

(42) A careful study which separates viscosity effects from electronic energy barriers during quenching of anthracene fluorescence has been made recently: Rice, J.; McDonald, D. B.; Ng, L.-K.; Yang, N. C. *J. Chem. Phys.* **1980**, *73*, 4144.

CM in directions perpendicular to the helical screw axis of the phase.

Conclusions

Detailed analysis of dynamic quenching data reveal that the preferred orientations for quenching pyrene singlets by a sterically hindered alkylamine, CA, in a nonpolar solvent, CM, is very specific and resembles closely the geometry (E) thought to be assumed by the corresponding exciplex.

Two separate methods for calculation of the activation parameters for pyrene singlet quenching in CM lead to very similar results: the activation energy in the cholesteric phase at low CA concentrations (E_6 = 9.9 ± 0.2 and 11.8 ± 0.7 kcal mol^{-1} by the two methods) is about twice that in the isotropic phase (E_6 = 5.3 ± 0.1 and 5.4 ± 1.4 kcal mol^{-1}). The entropy of activation in the cholesteric phase of CM is more positive than in the isotropic phase since the transition state is more disruptive of liquid crystalline order than are the dissociated reactants.

The magnitude of E_a(cholesteric) is *not* constant, but decreases with increasing CA concentration, approaching E_a(isotropic). The decrease is a consequence of CA disrupting the liquid crystalline order of CM, making the quenching transition state between pyrene and CA easier to attain.

Acknowledgment. We thank Dr. Dan Martire and the reviewers for their helpful suggestions. The National Science Foundation (Grant CHE-7906572) and the Naval Research Laboratory are acknowledged for their financial support of this research.

Appendix

As mentioned in the text, the method employed in calculating the activation parameters from the $d(\ln \tau)/d(1/T)$ slopes (Figure 2; column a and b of Table II) makes no assumptions concerning the reversibility of the pyrene–CA exciplex. The sole condition, that the pyrene decay times be much longer than those of the exciplex, is met. The second method employs the limiting Stern–Volmer slopes from Figure 4 with a quenching constant, $k_q = k_6$. If reverisiblity were significant, then eq 19 would hold. Substitution of Arrhenius expressions for k_6, k_7, and k_8 followed by differentiation of ln k_q yields eq 20.

$$k_q = k_6 k_8/(k_7 + k_8) \tag{19}$$

$$\frac{d \ln k_q}{d(1/T)} = \frac{-E_6}{R} - \frac{E_8}{R} + \frac{A_7E_7e^{-E_7/RT} + A_8E_8e^{-E_8/RT}}{R(A_7e^{-E_7/RT} + A_8e^{-E_8/RT})} \tag{20}$$

If reversibility is important, the activation energies in column c of Table II are equal to $E_6 + E_8 - (A_7E_7e^{-E_7/RT} + A_8E_8e^{-E_8/RT})/(A_7e^{-E_7/RT} + A_8e^{-E_8/RT})$. Therefore, $E_8 - (A_7E_7e^{-E_7/RT} + A_8E_8e^{-E_8/RT})/(A_7e^{-E_7/RT} + A_8e^{-E_8/RT})$ can be no larger than the difference between the activation energies in column c and either a or b.

That this difference is very small (and probably zero within the limits of *accuracy*) requires that either (1) $E_7 \simeq E_8$ or (2) $A_7E_7e^{-E_7/RT} \ll A_8E_8e^{-E_8/RT}$ and $A_7e^{-E_7/RT} \ll A_8e^{-E_8/RT}$. Any other condition would predict a temperature dependent value for the difference such that the Arrhenius slopes in Figure 5 would not be linear.

In the first case, reversibility is important and $k_7 \gg k_8$ because of entropy factors. Due to decreased solvent viscosity, exciplex dissociation increases with increasing temperature more rapidly than emission or nonradiative deactivation pathways.[22] Therefore, the correspondence between the activation energies in Table II ought to be much worse in the isotropic phase of CM than in its much more viscous cholesteric phase. In fact, the activation energies are equal.

The second condition makes exciplex formation irreversible: $k_7 \ll k_8$. In this case, $R[d \ln k_q/d(1/T)] = E_6$ and the activation energies calculated by the two methods should be very similar, as observed.

Photochemistry of the Tetranuclear Clusters $H_2Ru_4(CO)_{13}$, $H_2FeRu_3(CO)_{13}$, and $H_2FeOs_3(CO)_{13}$†

Henry C. Foley and Gregory L. Geoffroy*

Contribution from the Department of Chemistry, The Pennsylvania State University, University Park, Pennsylvania 16802. *Received May 17, 1981. Revised Manuscript Received August 10, 1981*

Abstract: Photolysis of $H_2FeRu_3(CO)_{13}$, $H_2Ru_4(CO)_{13}$, and $H_2FeOs_3(CO)_{13}$ in the presence of PPh_3 and H_2 leads to formation of the corresponding $H_2M_4(CO)_{12}(PPh_3)$ and $H_4M_4(CO)_{12}$ clusters with moderate efficiency. The 366-nm quantum yields for PPh_3 substitution are 0.030, 0.016, and 0.057, respectively. Photolysis of these clusters in the presence of CO leads to cluster fragmentation but with low quantum efficiency ($\phi \leq 10^{-5}$). The quantum yield for PPh_3 substitution in $H_2FeRu_3(CO)_{13}$ is independent of PPh_3 concentration but is decreased in the presence of added CO, implying competition of CO with PPh_3 for a photogenerated intermediate. The mechanism most consistent with all the experimental observations is one involving CO dissociation in the primary photochemical event, and not metal–metal bond homolysis.

Monomeric metal carbonyl complexes generally lose carbon monoxide upon photolysis whereas the dominant photoreaction for dinuclear carbonyls, such as $Mn_2(CO)_{10}$, is rupture of the metal–metal bond.[1] The latter process is believed to arise from excited states involving net population of metal–metal antibonding orbitals, depopulation of the corresponding bonding orbitals, or both.[1] Consider next metal carbonyl clusters which contain more than one metal–metal bond. Will these undergo net photofragmentation via metal–metal bond rupture with more or less efficiency than photoinduced CO dissociation? The reported spectral data for this class of compounds certainly indicates that the lowest-lying excited states are localized predominantly within the metal–metal bonded framework,[2-6] and thus photolysis would be

† Dedicated to George S. Hammond on the occasion of his 60th birthday.

(1) Geoffroy, G. L.; Wrighton, M. S. "Organometallic Photochemistry"; Academic Press: New York, 1979.

(2) Epstein, R. A.; Gaffney, T. R.; Geoffroy, G. L.; Gladfelter, W. L.; Henderson, R. S. *J. Am. Chem. Soc.* **1979**, *101*, 3847.

0002-7863/81/1503-7176$01.25/0